Appendix

9 Related Work

Jacot et al. [2018] showed the NTK to be the central quantity in the study of generalisation properties of infinite width DNNs. Jacot et al. [2019] identify two regimes that occur at initialisation in fully connected DNNs as the width increases to infinity namely i) *freeze:* here, the (scaled) NTK converges to a constant and hence leads to slow training, and ii) *chaos:* here, the NTK converges to Kronecker delta and hence hurts generalisation. Jacot et al. [2019] also suggest that for good generalisation it is important to operate the DNNs at the edge of the freeze and the chaos regimes. Arora et al. [2019] proposed pure kernel method based on the infinite width CNTK (NTK of convolutional neural network) and showed that it out performed state-of-the-art kernel methods by 10%. Arora et al. [2019] also noted a performance gain (about $5-6\%$) of the CNNs over the CNTK. However, it was also noted by Arora et al. [2019], Lee et al. [2019] that random NTFs obtained from finite width neural networks do not perform as well as their limiting infinite width counterparts. Arora et al. [2019], Cao and Gu [2019] provided generalisation bounds with the NTK norm. Du et al. [2018] use the NTK to show that over-parameterised DNNs trained by gradient descent achieve zero training error. Du and Hu [2019], Shamir [2019], Saxe et al. [2013] studied deep linear networks. Since deep linear networks are special cases of deep gated networks, Theorem 5.1 of our paper also provides an expression for the NTK at initialisation of deep linear networks. To see this, in the case of deep linear networks, all the gates are always 1 for all input examples, and Λ_Θ will be a matrix whose entries will be $w^{(d-1)}$.

The results in our paper are complementary to the prior NTF/NTK based works, in that, the NPK and NPFs are zeroth order kernel and features respectively. In contrast, the NTF is the gradient of the network output with respect to the weights of the network and hence the NTF/NTK are essentially first order quantities. The fixed NPF regime is different from the NTK regime and the freeze/chaos regimes studied in prior works, in that, in the fixed NPF setting the gates are controlled by a separate feature network.

Gated linearity was studied recently by Fiat et al. [2019], where single layered gated networks were considered. In terms of the work in our paper, Fiat et al. [2019] consider the fixed NPF setting with random NPFs of a single layer network. In contrast to the work by Fiat et al. [2019], in this paper we considered DGN of depth d, and we also showed (using the DNPFL setting) that by gradient descent on the parameters of the feature and the value network we can learn the NPFs leading to better generalisation than learning with the fixed random NPFs. We believe that handling of depth d networks, identification and the use of novel quantities namely NPFs, NPK and, the role of NPF learning in generalisation amount to significant progress in comparison to Fiat et al. [2019].

The role of gates was also empirically studied by Srivastava et al. [2014], where the active sub-networks are called as *locally competetive* networks. They encode the active subnetwork information in a sub-mask which is bit string that encodes the $0/1$ state of the all the gates. The sub-masks were then visualised using t-SNE. The visualisation showed that the "subnetworks active for examples of the same class are much more similar to each other compared to the ones activated for the examples of different classes". Balestriero et al. [2018] show the connection between $\max$-affine linearity and DNN with ReLU activations. Neyshabur et al. [2015] used the notion of paths to define a *path-norm* based gradient descent procedure.

A Expression for $K^{(d)}$

The $K^{(d)}$ matrix is computed by the recursion in (2).

$$\tilde{K}^{(1)}(s,s')=\Sigma^{(1)}(s,s')=\Sigma(s,s'), M^{(l)}_{ss'}=\begin{bmatrix}\Sigma^{(l)}(s,s) & \Sigma^{(l)}(s,s')\\ \Sigma^{(l)}(s',s) & \Sigma^{(l)}(s',s')\end{bmatrix}\in\mathbb{R}^2,$$

$$\Sigma^{(l+1)}(s,s')=2\cdot\mathbb{E}_{(q,q')\sim N(0,M^{(l)}_{ss'})}\left[\chi(q)\chi(q')\right], \hat{\Sigma}^{(l+1)}(s,s')=2\cdot\mathbb{E}_{(q,q')\sim N(0,M^{(l)}_{ss'})}\left[\partial\chi(q)\partial\chi(q')\right],$$

$$\tilde{K}^{(l+1)}=\tilde{K}^{(l)}\odot\hat{\Sigma}^{(l+1)}+\Sigma^{(l+1)}, K^{(d)}=\left(\tilde{K}^{(d)}+\Sigma^{(d)}\right)/2 \quad (2)$$

where $s, s' \in [n]$ are two input examples in the dataset, Σ is the data Gram matrix, $\partial\chi$ stands for the derivative of the activation function with respect to the pre-activation input, $N(0, M)$ stands for the mean-zero Gaussian distribution with co-variance matrix M.

B Experimental Setup

Dataset: We used standard datasets namely MNIST and CIFAR-10, with categorical cross entropy loss. We also used a 'Binary'-MNIST dataset, which is MNIST with only the two classes corresponding to digits 4 and 7, with label -1 for digit 4 and $+1$ for digit 7. For the 'Binary'-MNIST dataset, we used the squared loss.

Optimiser and Step-Size: We used stochastic gradient descent (SGD) and *Adam* as optimisers. In the case of SGD, we tried constant step-sizes in the set $\{0.1, 0.01, 0.001\}$ and chose the best. In the case of Adam the we used a constant step size of $3e^{-4}$. In both cases, we used batch size to be 32.

Network Architecture:

1. We used a fully connected (FC) DNN with $(w = 128, d = 5)$ for MNIST.

2. To train CIFAR-10, we used a *Vanilla* CNN architecture denoted by VCONV and a CNN architecture with *global-average-pooling* denoted by GCONV. VCONV is an architecture without pooling, residual connections, dropout or batch-normalisations, and is given by: input layer is $(32, 32, 3)$, followed by convolution layers with a stride of $(3, 3)$ and channels 64, 64, 128, 128 followed by a flattening to layer with 256 hidden units, followed by a fully connected layer with 256 units, and finally a 10 width soft-max layer to produce the final predictions. GCONV is same as VCONV with a *global-average-pooling* (GAP) layer at the boundary between the convolutional and fully connected layers.

Gating:

1. For both FRNPF, and FLNPF, we let $\chi^{\text{F}} = \chi_r$, and $G_{x,t}(l) = \gamma_r\left(q^{\text{F}}_{x,t}(l)\right)$.

2. In the case, DNPFL, we let $\chi^{\text{F}} = \chi_r$, and $G_{x,t}(l) = \gamma_{sr}\left(q^{\text{F}}_{x,t}(l)\right)$. Here $\gamma_{sr}(q) = \frac{1}{(1+\exp(-\beta \cdot q))}$ is a *soft-ReLU* gate which takes values in $(0, 1)$. In our experiments we used $\beta = 8$. The use of soft-ReLU makes it straightforward for the feature gradients to flow via the gating network.

Initialisation: In the case of FRNPF, we considered two possible initialisations namely i) *independent initialisation* (II), i.e., Θ^{F}_0 and Θ^{V}_0 are statistically independent, and ii) *dependent initialisation* (DI), i.e., $\Theta^{\text{F}}_0 = \Theta^{\text{V}}_0$, a case which mimics the NPFs and NPVs of a standard DNN with ReLU activations. In the case of FLNPF, $\Theta^{\text{F}}_0 = \bar{\Theta}$, where $\bar{\Theta}$ is the parameter of a pre-trained (at various stages of training) DNN with ReLU activations.

Epochs: All the models were trained close to 100% training accuracy. All the models took less than 100 epochs to train.

Reported Values: In order to obtain the values in Table 2, and in the left most plot of Figure 3 we used 5 runs. In each run, we took the best generalisation performance obtained in that run and then averaged the same over 5 runs.

C Applying Theorem 5.1 In Finite Width Case

In this section, we describe the technical step in applying Theorem 5.1 which requires $w \to \infty$ to measure the information in the gates of a DNN with finite width as per Definition 5.1. Since we are training only the value network in the FPNP mode of the DGN, it is possible to let the width of the value network alone go to ∞, while keeping the width of the feature network (which stores the fixed NPFs) finite. This is easily achieved by multiplying the width by a positive integer $m \in \mathbb{Z}_+$, and *padding* the gates 'm' times.

Definition C.1. *Define DGN$^{(m)}$ to be the DGN whose feature network is of width w and depth d, and whose value network is a fully connected network of width mw and depth d. The $mw(d-1)$ gating values are obtained by 'padding' the $w(d-1)$gating values of the width 'w', depth 'd' feature network 'm' times (see Figure 4, Table 3).*

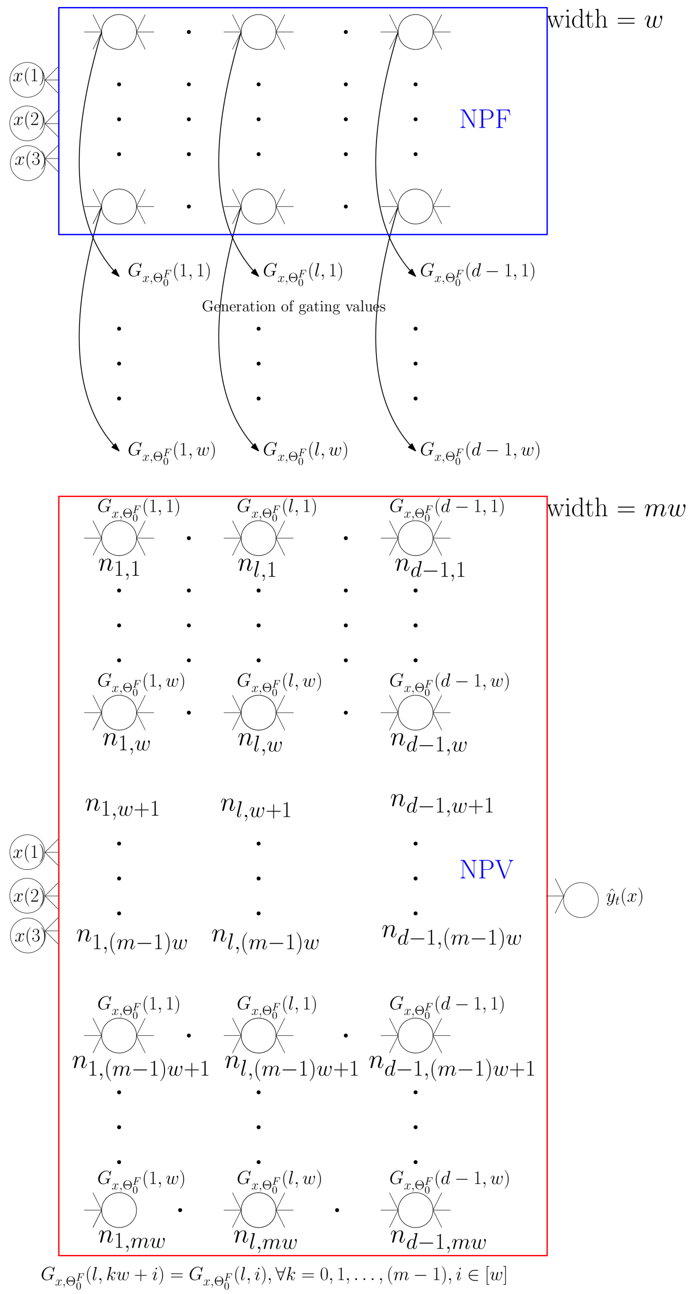

Figure 4: DGN$^{(m)}$ where the value network is of width mw and depth d. The gates are derived by padding the gating values obtained from the feature network 'm' times, i.e., $G_{x,t}(l, kw + i) = G_{x,t}(l, i), \forall k = 0, 1, \ldots, m-1, i \in [w]$.

Remark: DGN$^{(m)}$ has a total of $P^{(m)} = (mw)^{(d-1)} d_{in}$ paths. Thus, the NPF and NPV are quantities in $\mathbb{R}^{P^{(m)}}$. In what follows, we denote the NPF matrix of DGN$^{(m)}$ by $\Phi^{(m)}_{\Theta_0^{\mathrm{F}}} \in \mathbb{R}^{P^{(m)} \times n}$, and use $H^{(m)}_{\text{FNPF}} = (\Phi^{(m)}_{\Theta_0^{\mathrm{F}}})^\top \Phi^{(m)}_{\Theta_0^{\mathrm{F}}}$.

Before we proceed to state the version of Theorem 5.1 for DGN$^{(m)}$, we will look at an equivalent definition for Λ_Θ (see Definition 2.2).

Definition C.2. *For input examples $s, s' \in [n]$ define*

Layer	Feature Network (NPF)	Value Network (NPV)
Input	$z^{\text{F}}_{x,t}(0) = x$	$z^{\text{V}}_{x,t}(0) = x$
Activation	$q^{\text{F}}_{x,t}(l) = \Theta^{\text{F}}_t(l)^\top z^{\text{F}}_{x,t}(l-1)$	$q^{\text{V}}_{x,t}(l) = \Theta^{\text{V}}_t(l)^\top z^{\text{V}}_{x,t}(l-1)$
Hidden	$z^{\text{F}}_{x,t}(l) = \chi^{\text{F}}\left(q^{\text{F}}_{x,t}(l)\right)$	$z^{\text{V}}_{x,t}(l) = q^{\text{V}}_{x,t}(l) \odot G_{x,t}(l)$
Output	None	$\hat{y}_t(x) = \Theta^{\text{V}}(d)^\top z^{\text{V}}_{x,t}(d-1)$
Gating Values: $G_{x,t}(l) = \gamma_r\left(q^{\text{F}}_{x,t}(l)\right)$ or $G_{x,t}(l) = \gamma_{sr}\left(q^{\text{F}}_{x,t}(l)\right)$		

Table 3: Deep Gated Network with padding. Here the gating values are padded, i.e., $G_{x,t}(l, kw+i) = G_{x,t}(l,i), \forall k = 0, 1, \dots, m-1, i \in [w]$.

1. $\tau_\Theta(s,s',l) \stackrel{def}{=} \sum_{i=1}^{w} G_{x_s,\Theta}(l,i) G_{x_{s'},\Theta}(l,i)$ *be the number of activations that are "on" for both inputs* $s, s' \in [n]$ *in layer* $l \in [d-1]$.

2. $\Lambda_\Theta(s,s') \stackrel{def}{=} \Pi_{l=1}^{d-1} \tau_\Theta(s,s',l)$.

Corollary C.1 (Corollary to Theorem 5.1)**.** *Under Assumption 5.1 with σ replaced by $\sigma_{(m)} = \sigma/\sqrt{m}$, as $m \to \infty$, $K_{\Theta_0^{DGN(m)}} \to K^{(d)}_{FNPF} = d \cdot \sigma_{(m)}^{2(d-1)} H^{(m)}_{FNPF} = d \cdot \sigma^{2(d-1)} H_{FNPF}$.*

Proof. Let $\Lambda^{(m)}_{\text{FNPF}}$ and $\tau^{(m)}_{\text{FNPF}}$ be quantities associated with $\text{DGN}^{(m)}$. We know that $H^{(m)}_{\text{FNFP}} = \Sigma \odot \Lambda^{(m)}_{\text{FNPF}}$. Dropping the subscript FNPF to avoid notational clutter, we have

$$\begin{aligned}
\left(\sigma/\sqrt{m}\right)^{2(d-1)} \Lambda^{(m)}(s,s') &= \sigma^{2(d-1)} \frac{1}{m^{(d-1)}} \Pi_{l=1}^{d-1} \tau^{(m)}(s,s',l) \\
&= \sigma^{2(d-1)} \frac{1}{m^{(d-1)}} \Pi_{l=1}^{d-1} \left(m\tau(s,s',l)\right) \\
&= \sigma^{2(d-1)} \frac{1}{m^{(d-1)}} m^{(d-1)} \Pi_{l=1}^{d-1} \tau(s,s',l) \\
&= \sigma^{2(d-1)} \Pi_{l=1}^{d-1} \tau(s,s',l) \\
&= \sigma^{2(d-1)} \Lambda(s,s')
\end{aligned}$$

□

D Proofs of technical results

Proof of Proposition 1.1

Proof. We know that $e_t = (e_t(s), s \in [n]) \in \mathbb{R}^n$, and $e_t(s) = \hat{y}_{\Theta_t}(x_s) - y(s)$. Now

$$\begin{aligned}
L_{\Theta_t} &= \frac{1}{2} \sum_{s'=1}^{n} (\hat{y}_{\Theta_t} - y)^2 \\
&= \frac{1}{2} \sum_{s'=1}^{n} e_t^2 \\
\nabla_\Theta L_{\Theta_t} &= \sum_{s'=1}^{n} \nabla_\Theta \hat{y}_{\Theta_t}(x_{s'}) e_t(s') \\
\nabla_\Theta L_{\Theta_t} &= \sum_{s'=1}^{n} \psi_{x_{s'},\Theta_t} e_t(s') \qquad (3)
\end{aligned}$$

For gradient descent, $\dot{\Theta}_t = -\nabla_\Theta L_{\Theta_t}$, from (3) it follows that

$$\dot{\Theta}_t = -\sum_{s'=1}^{n} \psi_{x_{s'},\Theta_t} e_t(s') \qquad (4)$$

Now $\dot{e}_t = \dot{\hat{y}}_{\Theta_t}$, and expanding $\dot{\hat{y}}_{\Theta_t}(x_s)$ for some $s \in [n]$, we have:

$$\begin{aligned}\dot{\hat{y}}_{\Theta_t}(x_s) &= \frac{d\hat{y}_{\Theta_t}(x_s)}{dt}\\ &= \sum_{\theta\in\Theta}\frac{d\hat{y}_{\Theta_t}(x_s)}{d\theta}\frac{d\theta_t}{dt}, \text{ by expressing this summation as a dot product we obtain}\\ \dot{\hat{y}}_{\Theta_t}(x_s) &= \langle \psi_{x_s,\Theta_t}, \dot{\Theta}_t\rangle \end{aligned} \tag{5}$$

We now use that fact that Θ_t is updated by gradient descent

$$\begin{aligned}\dot{\hat{y}}_{\Theta_t}(x_s) &= -\langle \psi_{x_s,\Theta_t}, \sum_{s'=1}^{n}\psi_{x_{s'},\Theta_t} e_t(s')\rangle\\ &= -\sum_{s'=1}^{n} K_{\Theta_t}(s,s')e_t(s') \end{aligned} \tag{6}$$

The proof is complete by recalling that $\hat{y}_{\Theta_t} = (\hat{y}_{\Theta_t}(x_s), s\in[n])$, and $\dot{e}_t = \dot{\hat{y}}_{\Theta_t}$. □

Proof of Proposition 2.1

Proof. Let $x \in \mathbb{R}^{d_{in}}$ be the input to the DNN and $\hat{y}_\Theta(x)$ be its output. The output can be written in terms of the final hidden layer output

$$\begin{aligned}\hat{y}_\Theta(x) &= \Theta(d)^\top z_{x,\Theta}(d-1)\\ &= \sum_{j_{d-1}=1}^{w}\Theta(d,j_{d-1},1)z_{x,\Theta}(d-1,j_{d-1})\\ &= \sum_{j_{d-1}=1}^{w}\Theta(d,j_{d-1},1)G_{x\Theta}(d-1,j_{d-1})q_{x,\Theta}(d-1,j_{d-1}) \end{aligned} \tag{7}$$

Now $q_{x,\Theta}(d-1,j_{d-1})$ for a fixed j_{d-1} can again be expanded as

$$\begin{aligned}q_{x,\Theta}(d-1,j_{d-1}) &= \sum_{j_{d-2}=1}^{w}\Theta(d,j_{d-2},j_{d-1})z_{x,\Theta}(d-2,j_{d-2})\\ &= \sum_{j_{d-2}=1}^{w}\Theta(d-1,j_{d-2},j_{d-1})G_{x,\Theta}(d-2,j_{d-2})q_{x,\Theta}(d-2,j_{d-2}) \end{aligned} \tag{8}$$

Now plugging in (8) in the expression in (7), we have

$$\begin{aligned}\hat{y}_\Theta(x) &= \sum_{j_{d-1}=1}^{w}\Theta(d,j_{d-1},1)G_{x\Theta}(d-1,j_{d-1})\left(\sum_{j_{d-2}=1}^{w}\Theta(d-1,j_{d-2},j_{d-1})G_{x,\Theta}(d-2,j_{d-2})q_{x,\Theta}(d-2,j_{d-2})\right)\\ &= \sum_{j_{d-1},j_{d-2}\in[w]} G_{x,\Theta}(d-1,j_{d-1})G_{x,\Theta}(d-2,j_{d-2})\Theta(d,j_{d-1},1)\Theta(d-1,j_{d-2},j_{d-1})q_{x,\Theta}(d-2,j_{d-2}) \end{aligned} \tag{9}$$

By expanding q's for all the previous layers till the input layer we have

$$\sum_{j_d=1,j_{d-1},\ldots,j_1\in[w],j\in[d_{in}]} x(j)\Pi_{l=1}^{d-1}G_{x,\Theta}(l,j_l)\Pi_{l=1}^{d}\Theta(l,j_{l-1},j_l)$$

□

Proof of Lemma 2.1

Proof.

$$
\begin{aligned}
\langle \phi_{x_s,\Theta}, \phi_{x_{s'},\Theta} \rangle &= \sum_{p\in[P]} x_s(\mathcal{I}_0(p)) x_{s'}(\mathcal{I}_0(p)) A_\Theta(x_s,p) A_\Theta(x_{s'},p) \\
&= \sum_{i=1}^{d_{in}} x_s(i) x_{s'}(i) \Lambda_\Theta(s,s') \\
&= \langle x_s, x_{s'} \rangle \cdot \Lambda_\Theta(s,s') \qquad (10)
\end{aligned}
$$

□

Proof of Proposition 3.1

Proof. Let $\Psi_\Theta = (\psi_{x_s,\Theta}, s\in[n]) \in \mathbb{R}^{d_{net}\times n}$ be the NTF matrix, then the NTK matrix is given by $K_{\Theta_t} = \Psi^\top_{\Theta_t}\Psi_{\Theta_t}$. Note that, $\hat{y}_\Theta(x_s) = \langle \phi_{x_s,\Theta}, v_\Theta\rangle = \langle v_\Theta, \phi_{x_s,\Theta}\rangle = v^\top_\Theta \phi_{x_s,\Theta}$. Now $\psi_{x_s,\Theta} = \nabla_\Theta v_\Theta \phi_{x_s,\Theta}$, and hence $\Psi = \nabla_\Theta v_\Theta \Phi_\Theta$. Hence, $K_{\Theta_t} = \Psi^\top_{\Theta_t}\Psi_{\Theta_t} = \Phi^\top_\Theta (\nabla_\Theta v_\Theta)^\top (\nabla_\Theta v_\Theta)\Phi_\Theta = \Phi^\top_\Theta \mathcal{V}_\Theta \Phi_\Theta$. □

Proof of Proposition 3.2

Proof. Follows in a similar manner as the proof of Proposition 1.1. □

Proof of Proposition 3.3

Proof. $\rho_{\min}(K_\Theta) = \min_{\substack{x\in\mathbb{R}^n \\ \|x\|_2=1}} x^\top K_\Theta x$. Let $x'\in\mathbb{R}^n$ such that $\|x'\|_2 = 1$ and $\rho_{\min}(K_\Theta) = {x'}^\top K_\Theta x'$. Now, let $y' = \Phi x'$. Then we have, $\rho_{\min}(K_\Theta) = {y'}^\top \mathcal{V}_\Theta y'$. Hence $\rho_{\min}(K_\Theta) \le \|y'\|_2^2 \rho_{\max}(\mathcal{V}_\Theta)$. Now, $\|y'\|_2^2 = {x'}^\top \Phi^\top_\Theta \Phi_\Theta x' \le \rho_{min}(H_\Theta)$. □

Proof of Proposition 4.1

Proof. Follows in a similar manner as proof of Proposition 1.1. □

Lemma D.1. *Let $\varphi_{p,\Theta}$ be as in Definition 3.1, under Assumption 5.1, for paths $p, p_1, p_2 \in \mathcal{P}$, $p_1 \neq p_2$, at initialisation we have (i) $\mathbb{E}\left[\langle \varphi_{p_1,\Theta^{\mathrm{v}}_0}, \varphi_{p_2,\Theta^{\mathrm{v}}_0}\rangle\right] = 0$, (ii) $\langle \varphi_{p,\Theta^{\mathrm{v}}_0}, \varphi_{p,\Theta^{\mathrm{v}}_0}\rangle = d\sigma^{2(d-1)}$.*

Proof.

$$
\langle \varphi_{p_1,\Theta^{\mathrm{v}}_0}, \varphi_{p_2,\Theta^{\mathrm{v}}_0}\rangle = \sum_{\theta^{\mathrm{v}}\in\Theta^{\mathrm{v}}} \partial_{\theta^{\mathrm{v}}} v_{\Theta^{\mathrm{v}}_0}(p_1) \partial_{\theta^{\mathrm{v}}} v_{\Theta^{\mathrm{v}}_0}(p_2)
$$

Let $p \rightsquigarrow (\cdot)$ denote the fact that path p passes through $(\cdot)$, and let $p \not\rightsquigarrow (\cdot)$ denote the fact that path p does not pass through $\not\rightsquigarrow$. Let $\theta^{\mathrm{V}} \in \Theta^{\mathrm{V}}$ be any weight such that $p \rightsquigarrow \theta^{\mathrm{V}}$, and w.l.o.g let θ^{V} belong to layer $l'\in[d]$. If either $p_1 \not\rightsquigarrow \theta^{\mathrm{V}}$ or $p_2 \not\rightsquigarrow \theta^{\mathrm{V}}$, then it follows that $\partial_{\theta^{\mathrm{v}}} v_{\Theta^{\mathrm{v}}_0}(p_1)\partial_{\theta^{\mathrm{v}}} v_{\Theta^{\mathrm{v}}_0}(p_2) = 0$. In the case when $p_1, p_2 \rightsquigarrow \theta^{\mathrm{V}}$, we have

$$
\begin{aligned}
&\mathbb{E}\left[\partial_{\theta^{\mathrm{v}}} v_{\Theta^{\mathrm{v}}_0}(p_1)\partial_{\theta^{\mathrm{v}}} v_{\Theta^{\mathrm{v}}_0}(p_2)\right] \\
&= \mathbb{E}\left[\prod_{\substack{l=1\\ l\neq l'}}^{d} \left(\Theta^{\mathrm{V}}_0(l, \mathcal{I}_{l-1}(p_1), \mathcal{I}_l(p_1))\Theta^{\mathrm{V}}_0(l, \mathcal{I}_{l-1}(p_2), \mathcal{I}_l(p_2))\right)\right] \\
&= \prod_{\substack{l=1\\ l\neq l'}}^{d} \mathbb{E}\left[\Theta^{\mathrm{V}}_0(l, \mathcal{I}_{l-1}(p_1), \mathcal{I}_l(p_1))\Theta^{\mathrm{V}}_0(l, \mathcal{I}_{l-1}(p_2), \mathcal{I}_l(p_2))\right]
\end{aligned}
$$

where the $\mathbb{E}[\cdot]$ moved inside the product because at initialisation the weights (of different layers) are independent of each other. Since $p_1 \neq p_2$, in one of the layers $\tilde{l}\in[d-1], \tilde{l}\neq l'$ they do not pass through the same weight, i.e., $\Theta_0^{\mathrm{V}}(\tilde{l}, \mathcal{I}_{\tilde{l}-1}(p_1), \mathcal{I}_{\tilde{l}}(p_1))$ and $\Theta_0^{\mathrm{V}}(\tilde{l}, \mathcal{I}_{\tilde{l}-1}(p_2), \mathcal{I}_{\tilde{l}}(p_2))$ are distinct weights. Using this fact

$$\begin{aligned}
&\mathbb{E}\left[\partial_{\theta^{\mathrm{V}}} v_{\Theta_0^{\mathrm{V}}}(p_1)\partial_{\theta^{\mathrm{V}}} v_{\Theta_0^{\mathrm{V}}}(p_2)\right] \\
&= \prod_{\substack{l=1 \\ l\neq l', \tilde{l}}}^{d} \mathbb{E}\left[\Theta_0^{\mathrm{V}}(l, \mathcal{I}_{l-1}(p_1), \mathcal{I}_l(p_1))\Theta_0^{\mathrm{V}}(l, \mathcal{I}_{l-1}(p_2), \mathcal{I}_l(p_2))\right] \\
&= \mathbb{E}\left[\Theta_0^{\mathrm{V}}(\tilde{l}, \mathcal{I}_{\tilde{l}-1}(p_1), \mathcal{I}_{\tilde{l}}(p_1))\right]\mathbb{E}\left[\Theta_0^{\mathrm{V}}(\tilde{l}, \mathcal{I}_{\tilde{l}-1}(p_2), \mathcal{I}_{\tilde{l}}(p_2))\right] \\
&= 0
\end{aligned}$$

The proof of (ii) is complete by noting that $\sum_{\theta^{\mathrm{V}}\in\Theta^{\mathrm{V}}} \partial_{\theta^{\mathrm{V}}} v_{\Theta_0^{\mathrm{V}}}(p)\partial_{\theta^{\mathrm{V}}} v_{\Theta_0^{\mathrm{V}}}(p)$ has d non-zero terms for a single path p and at initialisation we have

$$\begin{aligned}
&\partial_{\theta^{\mathrm{V}}} v_{\Theta_0^{\mathrm{V}}}(p)\partial_{\theta^{\mathrm{V}}} v_{\Theta_0^{\mathrm{V}}}(p) \\
&= \prod_{\substack{l=1 \\ l\neq l'}}^{d} \Theta_0^{\mathrm{V}2}(l, \mathcal{I}_{l-1}(p), \mathcal{I}_l(p)) \\
&= \sigma^{2(d-1)}
\end{aligned}$$

□

Detailed version of Theorem 5.1 with proof.

Theorem D.1. *Under Assumption 5.1, and $\frac{4d}{w^2} < 1$ it follows that*

$$\begin{aligned}
\mathbb{E}\left[K_{\Theta_0^{DGN}}\right] &= d\cdot\sigma^{2(d-1)} H_{FNPF} \\
Var\left[K_{\Theta_0^{DGN}}(s,s')\right] &\leq O\left(d_{in}^2\sigma^{4(d-1)}\max\{d^2 w^{2(d-2)+1}, d^3 w^{2(d-2)}\}\right)
\end{aligned}$$

Proof. We have

$$\begin{aligned}
\mathbb{E}\left[K_{\Theta_0^{\mathrm{DGN}}}\right] &= \mathbb{E}\left[\Phi_{\mathrm{FNPF}}^\top \mathcal{V}_{\Theta_0^{\mathrm{V}}}\Phi_{\mathrm{FNPF}}\right] \\
&= \mathbb{E}\left[\Phi_{\mathrm{FNPF}}^\top (\nabla_{\Theta^{\mathrm{V}}} v_{\Theta_0^{\mathrm{V}}})^\top (\nabla_{\Theta^{\mathrm{V}}} v_{\Theta_0^{\mathrm{V}}})\Phi_{\mathrm{FNPF}}\right] \\
&= \Phi_{\mathrm{FNPF}}^\top \mathbb{E}\left[(\nabla_{\Theta^{\mathrm{V}}} v_{\Theta_0^{\mathrm{V}}})^\top (\nabla_{\Theta^{\mathrm{V}}} v_{\Theta_0^{\mathrm{V}}})\right]\Phi_{\mathrm{FNPF}} \\
&\overset{(a)}{=} d\cdot\sigma^{2(d-1)}\Phi_{\mathrm{FNPF}}^\top\Phi_{\mathrm{FNPF}} \\
&= d\cdot\sigma^{2(d-1)} H_{\mathrm{FNPF}}
\end{aligned}$$

where, (a) follows from Lemma D.1.

We now turn to the variance calculation. The idea is that we expand $Var\left[K_0(s,s')\right] = \mathbb{E}\left[K_0(s,s')^2\right] - \mathbb{E}\left[K_0(s,s')\right]^2$ and identify the terms which cancel due to subtraction and then bound the rest of the terms.

Notation: In what follows, we let K_0 to denote $K_{\Theta_0^{\mathrm{DGN}}}$ and drop superscript V from Θ_0^{V}, and subscript Θ_0^{V} from $v_{\Theta_0^{\mathrm{V}}}$. Further, we assume that the weights can be enumerated as $\theta(1), \dots, \theta(d_{net})$. We also denote $p \rightsquigarrow (\cdot)$ to denote the fact that path p passes through $(\cdot)$ and $p \not\rightsquigarrow (\cdot)$ to denote the fact that path p does not pass through $(\cdot)$. We use a shortcut notation $A(s,p)$ instead of $A(x_s,p)$. In what follows, we let $x \in \mathbb{R}^{d_{in}\times n}$ to be the data matrix.

Let $\theta(m), m \in [d_{net}]$ belong to layer $l'(m)$, then

$$
\begin{aligned}
&\mathbb{E}\left[K_0(s,s')\right] \\
&= \sum_{m=1}^{d_{net}} \mathbb{E}\left[\left(\sum_{p_1\in[P]} x(\mathcal{I}_0(p_1),s)A_0(s,p_1)\frac{\partial v_0(p_1)}{\partial\theta(m)}\right)\left(\sum_{p_2\in[P]} x(\mathcal{I}_0(p_2),s)A_0(s',p_2)\frac{\partial v_0(p_2)}{\partial\theta(m)}\right)\right] \\
&= \sum_{m=1}^{d_{net}} \mathbb{E}\left[\sum_{p_1,p_2\in[P]} x(\mathcal{I}_0(p_1),s)A_0(s,p_1)\frac{\partial v_0(p_1)}{\partial\theta(m)} x(\mathcal{I}_0(p_2),s')A_0(s',p_2)\frac{\partial v_0(p_2)}{\partial\theta(m)}\right] \\
&\overset{(a)}{=} \sum_{m=1}^{d_{net}} \sum_{\substack{p_1,p_2\in[P]\\ p_1,p_2\rightsquigarrow\theta(m)}} x(\mathcal{I}_0(p_1),s)A_0(s,p_1)x(\mathcal{I}_0(p_2),s')A_0(s',p_2)\mathbb{E}\left[\prod_{\substack{l=1\\ l\neq l'(m)}}^{d-1} \Theta_0(l,\mathcal{I}_{l-1}(p_1),\mathcal{I}_l(p_1))\right. \\
&\left.\Theta_0(l,\mathcal{I}_{l-1}(p_2),\mathcal{I}_l(p_2))\right] \\
&\overset{(b)}{=} \sum_{m=1}^{d_{net}} \sum_{\substack{p_1,p_2\in[P]\\ p_1,p_2\rightsquigarrow\theta(m)}} x(\mathcal{I}_0(p_1),s)A_0(s,p_1)x(\mathcal{I}_0(p_2),s')A_0(s',p_2) \prod_{\substack{l=1\\ l\neq l'(m)}}^{d-1} \mathbb{E}\Big[\Theta_0(l,\mathcal{I}_{l-1}(p_1),\mathcal{I}_l(p_1)) \\
&\Theta_0(l,\mathcal{I}_{l-1}(p_2),\mathcal{I}_l(p_2))\Big]
\end{aligned} \tag{11}
$$

where (a) follows from the fact that for $p \not\rightsquigarrow \theta(m)$, $\frac{\partial v_0(p)}{\partial\theta(m)} = 0$, and (b) follows from the fact that at initialisation the layer weights are independent of each other. Note that the right hand side of (11) only terms with $p_1 = p_2$ will survive the expectation.

In the following expression in (12), note that only terms of the form $p_1 = p_2$ and $p_3 = p_4$ are non-zero.

$$
\begin{aligned}
&\mathbb{E}\left[K_0(s,s')\right]^2 = \\
&\left(\sum_{m=1}^{d_{net}} \sum_{\substack{p_1,p_2\in[P]\\ p_1,p_2\rightsquigarrow\theta(m)}} x(\mathcal{I}_0(p_1),s)A_0(s,p_1)x(\mathcal{I}_0(p_2),s')A_0(s',p_2) \prod_{\substack{l=1\\ l\neq l'(m)}}^{d-1} \mathbb{E}\Big[\Theta_0(l,\mathcal{I}_{l-1}(p_1),\mathcal{I}_l(p_1))\right. \\
&\left.\Theta_0(l,\mathcal{I}_{l-1}(p_2),\mathcal{I}_l(p_2))\Big]\right)\times \\
&\left(\sum_{m'=1}^{d_{net}} \sum_{\substack{p_3,p_4\in[P]\\ p_3,p_4\rightsquigarrow\theta(m')}} x(\mathcal{I}_0(p_3),s)A_0(s,p_3)x(\mathcal{I}_0(p_4),s')A_0(s',p_4) \prod_{\substack{l=1\\ l\neq l'(m')}}^{d-1} \mathbb{E}\Big[\Theta_0(l,\mathcal{I}_{l-1}(p_3),\mathcal{I}_l(p_3))\right. \\
&\left.\Theta_0(l,\mathcal{I}_{l-1}(p_4),\mathcal{I}_l(p_4))\Big]\right)
\end{aligned}
$$

$$\mathbb{E}\left[K_0(s,s')\right]^2 = \sum_{m,m'=1}^{d_{net}} \sum_{\substack{p_1,p_2,p_3,p_4\in[P]\\ p_1,p_2\rightsquigarrow\theta(m)\\ p_3,p_4\rightsquigarrow\theta(m')}} \Bigg[\Bigg(x(\mathcal{I}_0(p_1),s)A_0(s,p_1)x(\mathcal{I}_0(p_2),s')A_0(s',p_2)x(\mathcal{I}_0(p_3),s)$$

$$A_0(s,p_3)x(\mathcal{I}_0(p_4),s')A_0(s',p_4)\Bigg) \times \Bigg(\prod_{\substack{l=1\\ l\neq l'(m')\\ l\neq l'(m)}}^{d-1} \mathbb{E}\left[\Theta_0(l,\mathcal{I}_{l-1}(p_1),\mathcal{I}_l(p_1))\Theta_0(l,\mathcal{I}_{l-1}(p_2),\mathcal{I}_l(p_2))\right]$$

$$\mathbb{E}\left[\Theta_0(l,\mathcal{I}_{l-1}(p_3),\mathcal{I}_l(p_3))\Theta_0(l,\mathcal{I}_{l-1}(p_4),\mathcal{I}_l(p_4))\right]\Bigg)\times$$

$$\left(\mathbb{E}\left[\Theta_0(l,\mathcal{I}_{l'(m')-1}(p_1),\mathcal{I}_{l'(m')}(p_1))\Theta_0(l,\mathcal{I}_{l'(m')-1}(p_2),\mathcal{I}_{l'(m')}(p_2))\right]\right)\times$$

$$\left(\mathbb{E}\left[\Theta_0(l,\mathcal{I}_{l'(m)-1}(p_3),\mathcal{I}_{l'(m)}(p_3))\Theta_0(l,\mathcal{I}_{l'(m)-1}(p_4),\mathcal{I}_{l'(m)}(p_4))\right]\right)\Bigg] \quad (12)$$

In the expression in (13), paths p_1,p_2,p_3,p_4 do not have constraints, and can be distinct.

$$\mathbb{E}\left[K_0^2(s,s')\right] = \sum_{m,m'=1}^{d_{net}} \sum_{\substack{p_1,p_2,p_3,p_4\in[P]\\ p_1,p_2\rightsquigarrow\theta(m)\\ p_3,p_4\rightsquigarrow\theta(m')}} \Bigg[\Bigg(x(\mathcal{I}_0(p_1),s)A_0(s,p_1)x(\mathcal{I}_0(p_2),s')A_0(s',p_2)x(\mathcal{I}_0(p_3),s)$$

$$A_0(s,p_3)x(\mathcal{I}_0(p_4),s')A_0(s',p_4)\Bigg) \times \Bigg(\prod_{\substack{l=1\\ l\neq l'(m')\\ l\neq l'(m)}}^{d-1} \mathbb{E}[\Theta_0(l,\mathcal{I}_{l-1}(p_1),\mathcal{I}_l(p_1))\Theta_0(l,\mathcal{I}_{l-1}(p_2),\mathcal{I}_l(p_2))$$

$$\Theta_0(l,\mathcal{I}_{l-1}(p_3),\mathcal{I}_l(p_3))\Theta_0(l,\mathcal{I}_{l-1}(p_4),\mathcal{I}_l(p_4))]\Bigg)\times$$

$$\left(\mathbb{E}\left[\Theta_0(l,\mathcal{I}_{l'(m')-1}(p_1),\mathcal{I}_{l'(m')}(p_1))\Theta_0(l,\mathcal{I}_{l'(m')-1}(p_2),\mathcal{I}_{l'(m')}(p_2))\right]\right)\times$$

$$\left(\mathbb{E}\left[\Theta_0(l,\mathcal{I}_{l'(m)-1}(p_3),\mathcal{I}_{l'(m)}(p_3))\Theta_0(l,\mathcal{I}_{l'(m)-1}(p_4),\mathcal{I}_{l'(m)}(p_4))\right]\right)\Bigg] \quad (13)$$

We now state the following facts/observations.

• *Fact 1:* Any term that survives the expectation (i.e., does not become 0) and participates in (13) is of the form $\sigma^{4(d-1)}\big(x(\mathcal{I}_0(p_1),s)A_0(s,p_1)x(\mathcal{I}_0(p_2),s')A_0(s',p_2)x(\mathcal{I}_0(p_3),s)A_0(s,p_3)x(\mathcal{I}_0(p_4),s')A_0(s',p_4)\big)$, where p_1,p_2,p_3,p_4 are free variables. Any term that survives the expectation (i.e., does not become 0) and participates in participates in (12) is of the form $\sigma^{4(d-1)}\big(x(\mathcal{I}_0(p_1),s)A_0(s,p_1)x(\mathcal{I}_0(p_2),s')A_0(s',p_2)x(\mathcal{I}_0(p_3),s)A_0(s,p_3)x(\mathcal{I}_0(p_4),s')A_0(s',p_4)\big)$, where $p_1=p_2, p_3=p_4$.

• *Fact 2:* The number of paths through a particular weight $\theta(m)$ in one of the middle layers is $d_{in}w^{d-3}$. The number of paths through a particular weight $\theta(m)$ in the first layer is w^{d-2} . The number of paths through a particular weight $\theta(m)$ in the last layer is $d_{in}w^{d-2}$.

• *Fact 3:* Let $\mathcal{P}'$ be an arbitrary set of paths constrained to pass through some set of weights. Let $\mathcal{P}''$ be the set of paths obtained by adding an additional constraint that the paths also should pass through a particular weight say $\theta(m)$. Now, if $\theta(m)$ belongs to :

1. a middle layer, then $|\mathcal{P}''| = \frac{|\mathcal{P}'|}{w^2}$.

2. the first layer, then $|\mathcal{P}''| = \frac{|\mathcal{P}'|}{d_{in} w}$.

3. the last layer, then $|\mathcal{P}''| = \frac{|\mathcal{P}'|}{w}$.

• *Fact 4:* For any p_1, p_2, p_3, p_4 combination that survives the expectation in (13) can be written as

$$\Big(x(\mathcal{I}_0(p_1), s)A_0(s, p_1)x(\mathcal{I}_0(p_2), s')A_0(s', p_2)x(\mathcal{I}_0(p_3), s)$$
$$A_0(s, p_3)x(\mathcal{I}_0(p_4), s')A_0(s', p_4)\Big)\times$$
$$\Big(\prod_{\substack{l=1 \\ l\neq l'(m') \\ l\neq l'(m)}}^{d-1} \mathbb{E}[\Theta_0(l, \mathcal{I}_{l-1}(p_1), \mathcal{I}_l(p_1))\Theta_0(l, \mathcal{I}_{l-1}(p_2), \mathcal{I}_l(p_2))$$
$$\Theta_0(l, \mathcal{I}_{l-1}(p_3), \mathcal{I}_l(p_3))\Theta_0(l, \mathcal{I}_{l-1}(p_4), \mathcal{I}_l(p_4))]\Big)\times$$
$$\Big(\mathbb{E}\left[\Theta_0(l, \mathcal{I}_{l'(m')-1}(p_1), \mathcal{I}_{l'(m')}(p_1))\Theta_0(l, \mathcal{I}_{l'(m')-1}(p_2), \mathcal{I}_{l'(m')}(p_2))\right]\Big)\times$$
$$\Big(\mathbb{E}\left[\Theta_0(l, \mathcal{I}_{l'(m)-1}(p_3), \mathcal{I}_{l'(m)}(p_3))\Theta_0(l, \mathcal{I}_{l'(m)-1}(p_4), \mathcal{I}_{l'(m)}(p_4))\right]\Big)$$

where $\rho_a \rightsquigarrow \theta(m)$ and $\rho_b \rightsquigarrow \theta(m')$ are what we call as *base* (case) paths.

• *Fact 5:* For any given base paths ρ_a and ρ_b there could be multiple assignments possible for p_1, p_2, p_3, p_4.

• *Fact 6:* Terms in (13), wherein, the base case is generated as $p_1 = p_2 = \rho_a$ and $p_3 = p_4 = \rho_b$ (or $p_1 = p_2 = \rho_b$ and $p_3 = p_4 = \rho_a$), get cancelled with the corresponding terms in (12).

• *Fact 7:* When the bases paths ρ_a and ρ_b do not intersect (i.e., do not pass through the same weight in any one of the layers), the only possible assignment is $p_1 = p_2 = \rho_a$ and $p_3 = p_4 = \rho_b$ (or $p_1 = p_2 = \rho_b$ and $p_3 = p_4 = \rho_a$), and such terms are common in (13) and (12), and hence do not show up in the variance term.

• *Fact 7:* Let base paths ρ_a and ρ_b intersect/cross at layer $l_1, \ldots, l_k, k \in [d-1]$, and let $\rho_a = (\rho_a(1), \ldots, \rho_a(k+1))$ where $\rho_a(1)$ is a sub-path string from layer 1 to l_1, and $\rho_a(2)$ is the sub-path string from layer $l_1 + 1$ to l_2 and so on, and $\rho_a(k+1)$ is the sub-path string from layer $l_k + 1$ to the output node. Then the set of paths that can occur in $\mathbb{E}\left[K_0(s, s')^2\right]$ are of the form:

1. $p_1 = p_2 = \rho_a, p_3 = p_4 = \rho_b$ (or $p_1 = p_2 = \rho_b, p_3 = p_4 = \rho_a$) which get cancelled in the $\mathbb{E}\left[K_0(s, s')\right]^2$ term.
2. $p_1 = \rho_a$, $p_3 = \rho_b$, $p_2 = (\rho_b(1), \rho_a(2), \rho_a(3), \ldots, \rho_a(k+1))$, $p_4 = (\rho_a(1), \rho_b(2), \rho_b(3), \ldots, \rho_b(k+1))$, which are obtained by *splicing* the base paths in various combinations. Note that for such spliced paths $p_1 \neq p_2$ and $p_3 \neq p_4$ and hence do not occur in the expression for $\mathbb{E}\left[K_0(s, s')\right]^2$ in (12).

• *Fact 8:* For k crossings of the base paths there are 4^{k+1} splicings possible, and those many terms are extra in the $\mathbb{E}\left[K_0(s, s')^2\right]$ expression in (13), when compared to the $\mathbb{E}\left[K_0(s, s')\right]^2$ expression in (12).

Upper Bound: We now enumerate various possible crossings of the base paths, and calculate an upper bound for the magnitude of the contribution of 'spliced' terms to the variance term using the *Fact 1* to *Fact 8*. In short, we find an upper bound for the those terms that do not get cancelled in the variance calculation. Further, without loss of generality we drop $x(\mathcal{I}_0(p))$ and $A(\cdot, \cdot)$ terms in this upper calculation.

Case 1**:** $k = 1$ crossing, in either first or last layer. There are $d_{in} w$ weights in the first layer and w weights in the last layer. The number of base path combinations passing through the first layer is $w^{d-2} \times w^{d-2}$. The number of base path combinations passing through the last layer is $(d_{in}w^{d-2}) \times (d_{in}w^{d-2})$. For each of these cases, m, m' could take $O(d^2)$ possible values. And the multiplication of the weights themselves contribute to $\sigma^{4(d-1)}$. Splicing of these base paths could be done in 4^2 ways. Putting them together we have

$$\begin{aligned}
&\sigma^{4(d-1)} \times (w) \times (d_{in}^2 \times w^{d-2} \times w^{d-2}) \times d^2 \times 4^2 \\
&+ \sigma^{4(d-1)} \times (d_{in}w) \times (w^{d-2} \times w^{d-2}) \times d^2 \times 4^2 \\
&\leq 32 d_{in}^2 \sigma^{4(d-1)} d^2 w^{2(d-2)+1}
\end{aligned}$$

Case 2**:** $k = 1$ crossing, in one of the middle layers. There are $w^2(d-2)$ weights in the middle layers. The number of base path combinations that pass through a given weight in the middle layers is $(d_{in}w^{d-3}) \times (d_{in}w^{d-3})$. For each of these cases, m, m' could take $O(d^2)$ possible values. And the multiplication of the weights themselves contribute to $\sigma^{4(d-1)}$. Splicing of these base paths could be done in 4^2 ways. Putting them together we have

$$\sigma^{4(d-1)} \times w^2(d-2) \times (d_{in}^2 \times w^{d-3} \times w^{d-3}) \times d^2 \times 4^2 \leq 16 d_{in}^2 \sigma^{4(d-1)} d^3 w^{2(d-3)}$$

Case 3**:** $k = 2$ crossings, one in the first layer and other in the last layer. So, we have

$$\sigma^{4(d-1)}(d_{in}w \times w) \times (w^{(d-3)} \times w^{(d-3)}) d^2 \times 4^3 \leq (32 d_{in}^2 \sigma^{4(d-1)} d^2 w^{2(d-2)+1}) \times (4w^{-1}),$$

Case 4**:** $k = 2$ crossings, first one in the first layer or the last layer, and the second one in the middle layer. This can be obtained by looking at the Case 1 and then adding the further restriction that the base paths should cross each other in the middle layer.

$$\begin{aligned}
&32 d_{in}^2 \sigma^{4(d-1)} d^2 w^{2(d-2)+1} \times w^2(d-2) \times w^{-2} \times w^{-2} \times 4 \\
&\leq (32 d_{in}^2 \sigma^{4(d-1)} d^2 w^{2(d-2)+1}) \times (4dw^{-2})
\end{aligned}$$

Case 5**:** $k = 2$ crossings, in the middle layer. This can be obtained by taking Case 2 and then adding the further restriction that the base paths should cross each other in the middle layer.

$$16 d_{in}^2 \sigma^{4(d-1)} d^3 w^{2(d-3)} \times w^2(d-2) \times w^{-2} \times w^{-2} \times 4 \leq (16 d_{in}^2 \sigma^{4(d-1)} d^3 w^{2(d-3)}) \times (4dw^{-2})$$

Case 6**:** $k = 3$ crossings, first one in the first layer or the last layer, and the other two in the middle layers. This can be obtained by considering Case 4 and then adding the further restriction that the base paths should cross each other in the middle layer.

$$(32 d_{in}^2 \sigma^{4(d-1)} d^2 w^{2(d-2)+1}) \times (4dw^{-2}) \times (4dw^{-2})$$

Case 7**:** $k = 3$ crossings, first two in the first and last layers and the third one in the middle layers. This can be obtained by considering Case 3 and then adding the further restriction that the base paths should cross each other in the middle layer.

$$(32 d_{in}^2 \sigma^{4(d-1)} d^2 w^{2(d-2)+1}) \times (4w^{-1}) \times (4dw^{-2})$$

Case 8**:** $k = 3$ crossings, in the middle layer. This can be obtained by considering Case 5 and then adding the further restriction that the base paths should cross each other in the middle layer.

$$(16 d_{in}^2 \sigma^{4(d-1)} d^3 w^{2(d-3)}) \times (4dw^{-2}) \times (4dw^{-2})$$

The cases can be extended in a similar way, increasing the number of crossings. Now, assuming $\frac{4d}{w^2} < 1$, the bounds in the various terms can be lumped together as below:

• We can add the bounds for Case 1, Case 4, Case 6 and other cases obtained by adding more crossings (one at a time) in the middle layer to Case 6. This gives rise to a term which is upper bounded by (for some constant $C > 0$):

$$C d_{in}^2 \sigma^{4(d-1)} d^2 w^{2(d-2)+1} \left(\frac{1}{1 - 4dw^{-2}} \right)$$

• We can add the bounds for Case 3, Case 7 and other cases obtained by adding more crossings (one at a time) in the middle layer to Case 6. This gives rise to a term which is upper bounded by

$$Cd_{in}^2\sigma^{4(d-1)}d^3w^{2(d-2)}\left(\frac{1}{1-4dw^{-2}}\right)$$

• We can add the bounds for Case 2, Case 5, Case 8 and other cases obtained by adding more crossings (one at a time) in the middle layer to Case 6. This gives rise to a term which is upper bounded by

$$Cd_{in}^2\sigma^{4(d-1)}d^2w^{2(d-2)}\left(\frac{1}{1-4dw^{-2}}\right)$$

Putting together we have the variance to be bounded by

$$Cd_{in}^2\sigma^{4(d-1)}\max\{d^2w^{2(d-2)+1}, d^3w^{2(d-2)}\},$$

for some constant $C > 0$. □

E DGN as a Lookup Table: Applying Theorem 5.1 to a pure memorisation task

In this section, we modify the DGN in Figure 2 into a memorisation network to solve a pure memorisation task. The objective of constructing the memorisation network is to understand the roles of depth and width in Theorem 5.1 in a simplified setting. In this setting, we show increasing depth till a point helps in training and increasing depth beyond it hurts training.

Definition E.1 (Memorisation Network/Task)**.** *Given a set of values $(y_s)_{s=1}^n \in \mathbb{R}$, a memorisation network (with weights $\Theta \in \mathbb{R}^{d_{net}}$) accepts $s \in [n]$ as its input and produces $\hat{y}_\Theta(s) \approx y_s$ as its output. The loss of the memorisation network is defined as $L_\Theta = \frac{1}{2}\sum_{s=1}^n(\hat{y}_\Theta(s) - y_s)^2$.*

Layer	Memorisation Network
Input	$z_t(0) = 1$
Activation	$q_{s,t}(l) = \Theta_t(l)^\top z_{s,t}(l-1)$
Hidden	$z_{s,t}(l) = q_{s,t}(l) \odot G_{s,t}(l)$
Output	$\hat{y}_t(s) = \Theta(d)^\top z_{s,t}(d-1)$

Table 4: Memorisation Network. The input is fixed and is equal to 1. All the internal variables depend on the index s and the parameter Θ_t. The gating values Gs are external and independent variables.

Fixed Random Gating: The memorisation network is described in Table 4. In a memorisation network, the gates are *fixed and random*, i.e., for each index $s \in [n]$, the gating values $G_{s,0}(l,i), \forall l \in [d-1], i \in [w]$ are sampled from $Ber(\mu), \mu \in (0,1)$ taking values in $\{0,1\}$, and kept fixed throughout training, i.e., $G_{s,t}(\cdot,\cdot) = G_{s,0}(\cdot,\cdot)\,\forall\, t \geq 0$. The input to the memorisation network is fixed as 1, and since the gating is fixed and random there is a separate random sub-network to memorise each target $y_s \in \mathbb{R}$. The memorisation network can be used to memorise the targets $(y_s)_{s=1}^n$ by training it using gradient descent by minimising the squared loss L_Θ. In what follows, we let K_0 and H_0 to be the NTK and NPK of the memorisation network at initialisation.

Performance of Memorisation Network: From Proposition 1.1 we know that as $w \to \infty$, the training error dynamics of the memorisation network follows:

$$\dot{e}_t = -K_0 e_t, \tag{14}$$

i.e., the spectral properties of K_0 (or H_0) dictates the rate of convergence of the training error to 0. In the case of the memorisation network with fixed and random gates, we can calculate $\mathbb{E}[K_0]$ explicitly.

Spectrum of H_0: The input Gram matrix Σ is a $n \times n$ matrix with all entries equal to 1 and its rank is equal to 1, and hence $H_0 = \Lambda_0$. We can now calculate the properties of Λ_0. It is easy to check that

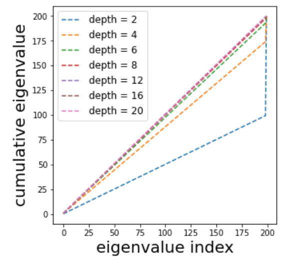

Figure 5: Ideal spectrum of $\mathbb{E}[K_0]/d$ for a memorisation network for $n = 200$.

$\mathbb{E}_\mu[\Lambda_0(s,s)] = (\mu w)^{(d-1)}, \forall s \in [n]$ and $\mathbb{E}_\mu[\Lambda_0(s,s')] = (\mu^2 w)^{(d-1)}, \forall s, s' \in [n]$. For $\sigma = \sqrt{\frac{1}{\mu w}}$, and $\mathbb{E}_\mu[K_0(s,s)/d] = 1$, and $\mathbb{E}_\mu[K_0(s,s')/d] = \mu^{(d-1)}$.

Why increasing depth till a point helps ? We have:

$$\frac{\mathbb{E}[K_0]}{d} = \begin{bmatrix} 1 & \mu^{d-1} & \dots & \mu^{d-1} & \dots \\ \dots & 1 & \dots & \mu^{d-1} & \dots \\ \dots & \mu^{d-1} & \dots & 1 & \dots \\ \dots & \mu^{d-1} & \dots & \mu^{d-1} & 1 \end{bmatrix} \tag{15}$$

i.e., all the diagonal entries are 1 and non-diagonal entries are μ^{d-1}. Now, let $\rho_i \geq 0, i \in [n]$ be the eigenvalues of $\frac{\mathbb{E}[K_0]}{d}$, and let $\rho_{\max}$ and $\rho_{\min}$ be the largest and smallest eigenvalues. One can easily show that $\rho_{\max} = 1 + (n-1)\mu^{d-1}$ and corresponds to the eigenvector with all entries as 1, and $\rho_{\min} = (1 - \mu^{d-1})$ repeats $(n-1)$ times, which corresponds to eigenvectors given by $[0, 0, \dots, \underbrace{1, -1}_{i \text{ and } i+1}, 0, 0, \dots, 0]^\top \in \mathbb{R}^n$ for $i = 1, \dots, n-1$. Note that as $d \to \infty$, $\rho_{\max}, \rho_{\min} \to 1$.

Why increasing depth beyond a point hurts? In Theorem D.1, note that for a fixed width w, as the depth increases the variance of the entries $K_0(s,s')$ deviates from its expected value $\mathbb{E}[K_0(s,s')]$. Thus the structure of the Gram matrix degrades from (15), leading to smaller eigenvalues.

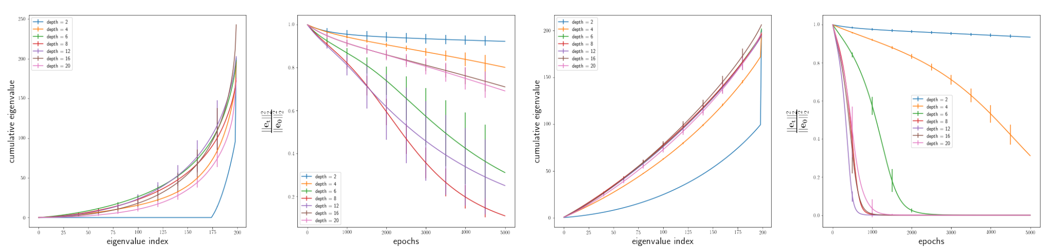

Figure 6: Shows the plots for the memorisation network with $\mu = \frac{1}{2}$ and $\sigma = \sqrt{\frac{2}{w}}$. The number of points to be memorised is $n = 200$. The left most plot shows the e.c.d.f for $w = 25$ and the second plot from the left shows the error dynamics during training for $w = 25$. The second plot from the right shows the e.c.d.f for $w = 500$ and the right most plot shows the error dynamics during training for $w = 500$. All plots are averaged over 10 runs.

E.1 Experiment

We set $n = 200$, and $y_s \sim \text{Uniform}[-1, 1]$. We look at the cumulative eigenvalue (e.c.d.f) obtained by first sorting the eigenvalues in ascending order then looking at their cumulative sum. The ideal behaviour (Figure 5) as predicted from theory is that for indices $k \in [n-1]$, the e.c.d.f should increase at a linear rate, i.e., the cumulative sum of the first k indices is equal to $k(1 - \mu^{d-1})$, and the difference between the last two indices is $1 + (n-1)\mu^{d-1}$. In Figure 6, we plot the actual e.c.d.f for various depths $d = 2, 4, 6, 8, 12, 16, 20$ and $w = 25, 500$ (first and third plots from the left in Figure 6).

Roles of depth and width: In order to compare how the rate of convergence varies with the depth, we set the step-size $\alpha = \frac{0.1}{\rho_{\max}}$, $w = 100$. We use the vanilla SGD-optimiser. Note the $\frac{1}{\rho_{\max}}$ in the stepsize, ensures that the uniformity of maximum eigenvalue across all the instances, and the convergence should be limited by the smaller eigenvalues. We also look at the convergence rate of the ratio $\frac{\|e_t\|_2^2}{\|e_0\|_2^2}$. We notice that for $w = 25$, increasing depth till $d = 8$ improves the convergence, however increasing beyond $d = 8$ worsens the convergence rate. For $w = 500$, increasing the depth till $d = 12$ improves convergence, and $d = 16, 20$ are worse than $d = 12$.